

Population Density Estimators for Right-Censored Distance Sampling

Wenzhe Huang¹, Guochun Shen², Dingliang Xing^{2,*}, Jiangyan Zhao^{3,†}

¹School of Mathematical Sciences, East China Normal University, Shanghai 200241, China

²School of Ecology and Environmental Science, East China Normal University, Shanghai 200241, China

³KLATASDS-MOE, School of Statistics, East China Normal University, Shanghai 200062, China

Abstract

Distance-based point-centered quarter method (PCQM) is widely used for population density estimation, yet its performance is challenged by right-censored observations arising from a truncated search radius. Existing methods for addressing such right-censored data are predominantly developed under the assumption of complete spatial randomness (CSR) using a Poisson model, while approaches for spatially aggregated populations—despite the negative binomial distribution (NBD) being well-established for uncensored distance sampling—remain lacking a systematic framework. This study presents a systematic set of censored distance-based estimators under these two core frameworks. We develop both moment-based estimators and maximum likelihood estimators (MLEs) under these two core frameworks, extending classical results to the censored setting for CSR populations and providing new inference tools for aggregated populations under the NBD model. Extensive simulations and applications to fully-censused forest plot data demonstrate that the NBD-based MLE achieves the highest accuracy and robustness across a wide range of ecological scenarios, with a median relative bias below 20% in most empirical scenarios—a level of estimation accuracy that cannot be consistently guaranteed by other competing methods, providing a rigorously validated toolkit for analyzing censored point-to-tree distance data.

Keywords: distance sampling; complete spatial randomness; spatial aggregation; negative binomial distribution; right-censored data; population density estimation; point-to-tree distances

*Corresponding author: ECNU-Alberta Joint Lab for Biodiversity Study, Zhejiang Tiantong Forest Ecosystem National Observation and Research Station, School of Ecology and Environmental Science, East China Normal University, Shanghai 200241, China, email: dlxing@des.ecnu.edu.cn

†The authors' names are listed in alphabetical order to reflect equal contribution.

1 Introduction

Population density is a fundamental ecological quantity underpinning studies of population dynamics, community structure, biodiversity assessment, and conservation planning (Cogbill, 2023; Santini et al., 2024). Accurate estimation of density is therefore central to both ecological inference and management decisions. For sessile organisms such as trees, distance-based sampling methods are particularly useful because they substantially reduce field effort relative to quadrat-based surveys while retaining analytical simplicity and interpretability. Among these methods, the point-centered quarter method (PCQM) has been widely adopted in forest ecology and vegetation surveys for several decades (Cottam and Curtis, 1956; Mitchell, 2007).

Classical PCQM density estimators were developed under the assumption of complete spatial randomness (CSR), typically represented by a homogeneous Poisson point process (Cottam et al., 1953; Morisita, 1954). Under this assumption, simple moment-based estimators yield closed-form expressions for population density based on point-to-tree distances. However, natural populations rarely conform to CSR. Spatial aggregation is common in ecological systems due to limited dispersal, conspecific attraction, disturbance regimes, and environmental heterogeneity. When such clustering is present, Poisson-based distance estimators are well known to systematically underestimate true population density (Pollard, 1971; He et al., 1997). To address this limitation, a range of alternative estimators has been proposed, culminating in recent developments that model point-to-tree distances using the negative binomial distribution (NBD). These NBD-based estimators provide a principled parametric framework for accommodating spatial aggregation and have been shown to substantially improve robustness over CSR-based methods in uncensored sampling settings (Shen et al., 2020; Stoklosa et al., 2022).

Despite these advances, an important and pervasive feature of field sampling has received comparatively little attention: right-censoring induced by a truncated search radius. In practice, PCQM surveys often impose a maximum search distance to maintain efficiency, ensure observer safety, or reflect limited visibility in dense vegetation or complex terrain (Levine et al., 2017; Cogbill, 2023). When no individual is detected within this predefined radius, the corresponding quarter is effectively right-censored. Such censored observations are common in forest surveys, particularly in low-density stands or highly aggregated populations (Warde and Petranka, 1981). Existing correction methods for censored PCQM data were largely developed under the CSR assumption (Warde and Petranka, 1981; Dahdouh-Guebas and Koedam, 2006) and consequently perform poorly when applied to aggregated spatial patterns (Mitchell, 2007). Notably, although NBD-based estimators have demonstrated strong performance for uncensored point-to-tree distances (Shen et al., 2020), no systematic framework currently integrates NBD modeling with right-censored distance sampling.

In this study, we address this gap by developing a unified set of population density estimators for right-censored PCQM data under two canonical spatial point process models: the Poisson model and the negative binomial model. For the Poisson case, we extend classical moment-based estimators to explicitly account for right-censoring and derive the corresponding maximum likelihood estimator. For the aggregation case, we propose new moment-based and likelihood-based estimators under the NBD framework that jointly accommodate spatial clustering and truncated observations. Together, these methods constitute the first comprehensive treatment of censored PCQM data that is valid under both random and aggregated spatial structures.

We evaluate the proposed estimators through extensive simulation studies and applications to fully mapped forest plot data. Across a wide range of ecological scenarios, results show that NBD-based likelihood estimators achieve consistently high accuracy and robustness, particularly when spatial aggregation and right-censoring occur simultaneously. By explicitly linking realistic field constraints with flexible spatial models, this work advances distance-based density estimation under practical survey conditions and provides ecologists with a rigorously validated toolkit for analyzing censored point-to-tree distance data.

2 Existing Estimators for Complete Data

We begin by reviewing existing population density estimators for complete (i.e., uncensored) point-to-individual distance data, which provide the methodological foundation for our subsequent development of estimators under right-censoring. Consider a standard point-centered quarter sampling design in which n sampling locations are independently selected within a study region. At each location, the surrounding space is partitioned into q equal-angle sectors, and the distance $r_{\ell ij}$ from the i th sampling point ($i = 1, \dots, n$) to the ℓ th nearest individual ($\ell = 1, 2, \dots$) within the j th sector ($j = 1, \dots, q$) is recorded. This design yields a total of nq observed distances, which we denote by $\{r_m : m = 1, \dots, nq\}$ for notational simplicity.

Distance-based density estimators derived from these observations depend critically on assumptions about the underlying spatial point process. In what follows, we summarize the principal estimators developed under two canonical models widely used in ecological applications: complete spatial randomness (CSR), represented by the Poisson model, and spatial aggregation, represented by the negative binomial distribution (NBD) model.

2.1 Poisson (CSR) case

Under the assumption of complete spatial randomness, the spatial locations of individuals follow a homogeneous Poisson point process. The Poisson model can also be viewed as a limiting case of the negative binomial model as the aggregation parameter $k \rightarrow \infty$ (Eberhardt, 1967). Under CSR, the probability density function of the distance R to the ℓ th nearest individual within each of the q equal-angle sectors is

$$f(r; \lambda) = \frac{2\pi\lambda r}{q} \frac{(\lambda\pi r^2/q)^{\ell-1}}{(\ell-1)!} \exp(-\lambda\pi r^2/q), \quad (1)$$

where λ denotes the population density.

Based on this distribution, a variety of classical density estimators have been proposed. Following the classification of Cogbill et al. (2018), two widely used forms are the Cottam-type and Pollard-type estimators. The Cottam-type estimator, originally generalized by Morisita (1954), is given by

$$\hat{\lambda}_C = \frac{q\ell}{4 \left[\frac{1}{nq} \sum_{m=1}^{nq} r_m \right]^2}, \quad (2)$$

which is based on the mean of observed distances. In contrast, the Pollard-type estimator (Morisita, 1957) exploits the second moment of the distances and is given by

$$\hat{\lambda}_P = \frac{q(nq\ell - 1)}{\pi \sum_{m=1}^{nq} r_m^2}. \quad (3)$$

From a likelihood perspective, the maximum likelihood estimator (MLE) of λ under CSR can be derived directly from (1), yielding

$$\hat{\lambda}_{\text{MLE}} = \frac{nq^2\ell}{\pi \sum_{m=1}^{nq} r_m^2}. \quad (4)$$

Although this estimator arises naturally from the likelihood, it is generally dominated by the Pollard-type estimator (3) due to its bias properties (Pollard, 1971), and is therefore rarely used in practice.

2.2 Negative binomial (aggregation) case

The accuracy of Poisson-based distance estimators depends critically on the assumption of CSR, which is frequently violated in ecological systems where individuals exhibit spatial aggregation. Such aggregation may arise from limited dispersal, habitat heterogeneity, or biological inter-

actions, and can lead to substantial underestimation of population density when CSR-based estimators are applied.

Early attempts to address aggregation in distance sampling include the estimators proposed by [Morisita \(1957\)](#), which rely on assumptions of local randomness within sectors even when the global spatial pattern is aggregated. Under this framework, Morisita proposed two estimators based on point-to-tree distances:

$$\hat{\lambda}_{m1} = \frac{\ell - 1}{\pi n} \sum_{m=1}^{nq} \frac{1}{r_m^2}, \quad (5)$$

which requires $\ell > 1$, and

$$\hat{\lambda}_{m2} = \frac{\ell q - 1}{\pi n} \sum_{i=1}^n \frac{q}{\sum_{j=1}^q r_{ij}^2}. \quad (6)$$

Comprehensive evaluations by [Cogbill et al. \(2018\)](#) indicate that these estimators remain among the best-performing classical plotless methods when CSR is violated.

A major advance was introduced by [Shen et al. \(2020\)](#), who explicitly modeled spatial aggregation using the negative binomial distribution. Although the NBD has long been recognized as a flexible model for aggregated spatial patterns ([Zillio and He, 2010](#); [Chen et al., 2018](#)), earlier applications to distance sampling often required numerical inversion or simulation-based procedures ([Eberhardt, 1967](#); [Gao, 2013](#)). In contrast, [Shen et al. \(2020\)](#) derived closed-form moment-based estimators, enabling direct and computationally efficient density estimation.

Under the NBD model, the probability density function of the distance R to the ℓ th nearest individual in each sector is

$$g(r; \lambda, k) = \frac{2(\pi \lambda q^{-1})^\ell r^{2\ell-1} \Gamma(\ell + k)}{k^\ell \Gamma(k) \Gamma(\ell)} \left(1 + \frac{\pi \lambda q^{-1} r^2}{k}\right)^{-\ell-k}, \quad (7)$$

where λ denotes population density and k controls the degree of spatial aggregation ([Shen et al., 2020](#)). The u th moment of R is given by

$$\mathbb{E}[R^u] = \left(\frac{kq}{\pi \lambda}\right)^{u/2} \frac{\Gamma(\ell + \frac{u}{2}) \Gamma(k - \frac{u}{2})}{\Gamma(\ell) \Gamma(k)}, \quad -2\ell < u < 2k.$$

When $u = -2$, this expression reduces to Morisita's first estimator (5), as shown by [Eberhardt \(1967\)](#). For $u = 2$, the second moment simplifies to $\mathbb{E}[R^2] = \frac{k\ell q}{\pi \lambda (k-1)}$, which requires $k > 1$.

Combining moment conditions based on $\mathbb{E}[R^{-1}]$, $\mathbb{E}[R]$, and $\mathbb{E}[R^2]$, [Shen et al. \(2020\)](#) de-

rived the NBD-based density estimator

$$\hat{\lambda}_n = \frac{q(2\ell - 1) \sum_{m=1}^{nq} r_m^{-1}}{\pi \sum_{m=1}^{nq} r_m} - \frac{nq^2 \ell}{\pi \sum_{m=1}^{nq} r_m^2}, \quad (8)$$

along with the corresponding estimator of the aggregation parameter,

$$\hat{k}_n = 1 - \frac{(\sum_{m=1}^{nq} r_m) \ell}{(\sum_{m=1}^{nq} r_m^{-1}) (\sum_{m=1}^{nq} r_m^2)^{\frac{1-2\ell}{nq}} + (\sum_{m=1}^{nq} r_m) \ell}. \quad (9)$$

Alternatively, likelihood-based estimation under the NBD model can be performed by maximizing the likelihood function

$$\mathcal{L}(\lambda, k) = \prod_{m=1}^{nq} g(r_m; \lambda, k),$$

with respect to λ and k . Because this likelihood does not admit closed-form solutions, numerical optimization is generally required. These likelihood-based estimators serve as important benchmarks and motivate our subsequent extension to right-censored distance data.

3 Improved Estimators for Right-censored Data

3.1 Poisson (CSR) case

In practical field surveys, distance sampling is often constrained by limited time, manpower, or visibility, necessitating the use of a fixed maximum search radius C . When recording distances to the ℓ th nearest individual in each of q sectors, sectors in which fewer than ℓ individuals are detected within radius C are recorded as right-censored observations (i.e., $R > C$). Such censored sectors are common in low-density stands or highly heterogeneous habitats, and ignoring them has been shown to induce positive bias in density estimation ([Warde and Petranka, 1981](#)).

Let n_0 denote the number of censored sectors, $\{r'_t : t = 1, 2, \dots, nq - n_0\}$ the set of fully observed distances, and $p_0 = n_0/(nq)$ the proportion of censored observations. Existing correction methods for censored PCQM data have largely been developed under the assumption of CSR ([Mitchell, 2007](#)). For the special case $\ell = 1$, [Warde and Petranka \(1981\)](#) proposed a correction factor based on the censored proportion p_0 , yielding the estimator

$$\hat{\lambda}_{\text{WP}} = \frac{q}{\pi \left(\frac{1}{nq - n_0} \sum_{t=1}^{nq - n_0} r'_t \right)^2} \cdot \frac{[\gamma(\frac{3}{2}, -\ln(p_0))]^2}{(1 - p_0)^2}, \quad (10)$$

where $\gamma(a, x) = \int_0^x t^{a-1} e^{-t} dt$ denotes the lower incomplete gamma function. Subsequently, [Dahdouh-Guebas and Koedam \(2006\)](#) proposed a simpler empirical correction,

$$\widehat{\lambda}_{\text{DK}} = \frac{q}{4 \left(\frac{1}{nq-n_0} \sum_{t=1}^{nq-n_0} r'_t \right)^2} (1 - p_0), \quad (11)$$

which performs reasonably well in practice despite lacking formal theoretical justification.

To generalize moment-based density estimation under CSR to right-censored data, we replace the conventional empirical moments with censoring-adjusted moments. Specifically, for any real number u , the complete-data sample moment $\frac{1}{nq} \sum_{m=1}^{nq} r_m^u$ is replaced by

$$M_u = \frac{\frac{1}{nq} \sum_{t=1}^{nq-n_0} r'_t{}^u \cdot \Gamma\left(\ell + \frac{u}{2}\right)}{\gamma\left(\ell + \frac{u}{2}, \widehat{m}_C\right)},$$

where \widehat{m}_C solves $\gamma(\ell, \widehat{m}_C)/\Gamma(\ell) = 1 - p_0$. When the maximum search radius C is sufficiently large, M_u reduces to the standard empirical moment (see Appendix SM: Section S1).

Applying these adjusted moments, the Cottam-type estimator (2) extends naturally to

$$\widehat{\lambda}_C^{(c)} = \frac{q\ell}{4(M_1)^2}, \quad (12)$$

and the Pollard-type estimator (3) becomes

$$\widehat{\lambda}_P^{(c)} = \frac{nq\ell - 1}{\pi n M_2}. \quad (13)$$

Notably, when $\ell = 1$, the censored Cottam-type estimator (12) reduces exactly to the Warde-Petran estimator (10). These estimators therefore provide consistent density estimates under CSR while explicitly accounting for right-censoring.

Likelihood-based estimation under CSR can also be extended to censored data. For $nq - n_0$ observed distances $\{r'_t\}$ and n_0 censored sectors, the likelihood function is

$$\mathcal{L}(\lambda) = \prod_{t=1}^{nq-n_0} f(r'_t; \lambda) [1 - F(C; \lambda)]^{n_0}, \quad (14)$$

where $f(\cdot)$ is given in (1) and

$$F(C; \lambda) = \frac{\gamma(\ell, \pi \lambda C^2 / q)}{\Gamma(\ell)}.$$

The maximum likelihood estimator $\widehat{\lambda}_{\text{MLE}}^{(c)}$ is obtained numerically for general ℓ . In the special case $\ell = 1$, the MLE admits a closed-form solution, which reduces to (4) as $n_0 = 0$.

$$\widehat{\lambda}_{\text{MLE}}^{(c)} = \frac{q(nq - n_0)}{\pi \left(\sum_{t=1}^{nq-n_0} r_t'^2 + n_0 C^2 \right)}. \quad (15)$$

3.2 Negative binomial (aggregation) case

We next extend the negative binomial distribution (NBD) framework to right-censored distance sampling, allowing spatial aggregation and truncation to be handled simultaneously. The core idea is to construct adjusted sample moments by replacing right-censored distances with their conditional expectation given the truncation threshold. For computational tractability and robust performance across aggregation levels, we approximate this conditional expectation under the complete spatial randomness (CSR) assumption. This CSR-based approximation is formally justified in Appendix SM: Section S2, where we show that the resulting bias is negligible under moderate censoring and vanishes as k increases. To adjust sample moments in the presence of censoring, we define

$$\widehat{\mathbb{E}[R^u]} = \frac{1}{nq} \left[\sum_{t=1}^{nq-n_0} r_t'^u + n_0 \mathbb{E}(R^u \mid R > C; k = \infty, \lambda = \lambda_{\text{init}}) \right],$$

where the conditional expectation for censored observations is

$$\mathbb{E}(R^u \mid R > C) = \left(\frac{q}{\pi \lambda_{\text{init}}} \right)^{u/2} \frac{\Gamma\left(\ell + \frac{u}{2}, \frac{\pi \lambda_{\text{init}} C^2}{q}\right)}{\Gamma\left(\ell, \frac{\pi \lambda_{\text{init}} C^2}{q}\right)}.$$

Here, $\Gamma(a, x)$ denotes the upper incomplete gamma function, and λ_{init} is an initial density estimate obtained from any censored-data estimator, including (11), (12), or (13).

Using these adjusted moments, the NBD-based density estimator (8) extends to

$$\widehat{\lambda}_n^{(c)} = \frac{q(2\ell - 1)\widehat{\mathbb{E}[R^{-1}]} - \frac{q\ell}{\pi\widehat{\mathbb{E}[R^2]}}}{\pi\widehat{\mathbb{E}[R]}}, \quad (16)$$

and Morisita's first estimator (5) becomes

$$\widehat{\lambda}_{m1}^{(c)} = \frac{q(\ell - 1)}{\pi} \widehat{\mathbb{E}[R^{-2}]}.$$
 (17)

These estimators enable the application of NBD-based methods, known to perform well under aggregation, to censored distance data commonly encountered in field surveys.

Finally, likelihood-based estimation under the NBD model can be extended to right-censored data. For $nq - n_0$ observed distances and n_0 censored sectors, the likelihood is

$$\mathcal{L}(\lambda, k) = \prod_{t=1}^{nq-n_0} g(r'_t; \lambda, k) [1 - F(C; \lambda, k)]^{n_0}, \quad (18)$$

where $g(\cdot)$ is given in (7). The cumulative distribution function is

$$F(C; \lambda, k) = I_w(\ell, k), \quad w = \frac{\pi\lambda C^2}{\pi\lambda C^2 + qk},$$

with $I_w(\cdot, \cdot)$ denoting the regularized incomplete beta function. The maximum likelihood estimators $\hat{\lambda}_{n, \text{MLE}}^{(c)}$ and $\hat{k}_{n, \text{MLE}}^{(c)}$ are obtained numerically by maximizing the corresponding log-likelihood.

4 Study design and evaluation criteria

We evaluated the performance of the proposed population density estimators for right-censored distance sampling using both simulated spatial point patterns and fully mapped forest plots. The simulation study was designed to span a broad range of spatial structures commonly encountered in ecological populations, from complete spatial randomness to strong aggregation, while the empirical analyses assessed estimator behavior under realistic forest conditions.

4.1 Simulation study

Two classes of spatial point processes were considered.

Complete spatial randomness (CSR). CSR populations were generated from homogeneous Poisson point processes (Thomas, 1949), representing the classical assumption underlying traditional plotless distance estimators. These simulations provide a baseline against which the performance of censored estimators can be evaluated under ideal conditions. Three population densities were examined, $\lambda_{\text{CSR}} = 0.005, 0.01, \text{ and } 0.05$ individuals per unit area, corresponding to sparse to moderately dense populations typical of ecological field surveys.

Under the CSR assumption, we compared four Poisson-based estimators:

1. the Dahdouh-Guebas and Koedam estimator, $\hat{\lambda}_{\text{DK}}$ (11), applicable when only the nearest neighbor ($\ell = 1$) is recorded;

2. the censored Cottam-type estimator, $\hat{\lambda}_C^{(c)}$ (12);
3. the censored Pollard-type estimator, $\hat{\lambda}_P^{(c)}$ (13);
4. the maximum likelihood estimator under CSR, $\hat{\lambda}_{\text{MLE}}^{(c)}$, based on the censored likelihood in (14).

This comparison isolates the relative efficiency and robustness of Poisson-based methods when their underlying assumptions are satisfied.

Aggregated (non-CSR) populations. To represent spatial aggregation arising from ecological processes such as limited dispersal, clonal growth, or habitat heterogeneity, we simulated Thomas cluster processes (Thomas, 1949). The overall population density was fixed at $\lambda_{\text{agg}} = 0.05$, matching the highest CSR density, while clustering strength was controlled through the cluster scale parameter σ . Parent intensity was set to $\kappa = \lambda_{\text{agg}}/\mu$ with $\mu = 5$ offspring per parent, and σ varied from 1.0 to 5.5 units in increments of 0.5. Smaller values of σ produce strongly aggregated patterns, whereas larger values approach spatial randomness.

For these aggregated populations, we evaluated three estimators derived under the negative binomial distance (NBD) framework:

1. the censored Shen-type estimator, $\hat{\lambda}_n^{(c)}$ (16);
2. the censored Morisita-type estimator, $\hat{\lambda}_{m1}^{(c)}$ (17);
3. the NBD-based maximum likelihood estimator, $\hat{\lambda}_{n,\text{MLE}}^{(c)}$, defined by (18).

These methods explicitly account for spatial aggregation and are expected to outperform Poisson-based estimators when clustering is present.

For each combination of process parameters, 10 independent point pattern realizations were generated in a 600×600 unit square study window using the `spatstat` package in R (Baddeley et al., 2015). Within each realization, we implemented a point-centered quarter method (PCQM) sampling design with $n = 120$ sampling points, $q = 4$ quadrants per point, and nearest-neighbor orders $\ell = 1, 2$, and 3. To reflect realistic field limitations, a maximum search radius of $C = 10$ units was imposed, with distances exceeding this threshold treated as right-censored observations. Sampling locations were generated using Latin hypercube sampling via the `lhs` package (Carnell, 2026) within a buffered study window, ensuring a minimum distance of $C + 0.1$ units from the boundary to avoid edge effects (Olsson et al., 2003). For each point pattern, 200 independent sets of sampling locations were generated to quantify variability due to sampling placement.

4.2 Empirical forest data

To assess performance under realistic ecological conditions, we applied all seven estimators to two fully censused forest dynamics plots: the 50-ha Barro Colorado Island (BCI) plot in Panama (Hubbell et al., 1986) and the 35-ha Harvard Forest plot in Massachusetts, USA (Foster, 1992). These datasets encompass a wide range of species abundances and spatial structures, including strong aggregation and habitat-driven heterogeneity.

For each species with at least 500 individuals, PCQM sampling was simulated with $n = 120$ sampling points and $q = 4$ quadrants. We considered four maximum search radii ($C = 10, 20, 30,$ and 40 m) and three nearest-neighbor orders ($\ell = 1, 2, 3$). Sampling points were generated using Latin hypercube sampling with a buffer of $C + 0.1$ m to avoid edge effects. For each species and parameter combination, 200 independent sampling designs were generated. True species densities were computed directly from the full census, allowing direct calculation of the same performance metrics used in the simulation study.

4.3 Performance metrics

Estimator performance was evaluated using relative error metrics calculated across the 200 sampling replicates for each scenario. Let $\hat{\lambda}_s$ denote the estimated density from the s -th replicate and λ_{true} the true population density, computed as the total number of points divided by the study area. Relative bias (rBias) measures systematic deviation,

$$\text{rBias} = \frac{1}{\lambda_{\text{true}}} \left(\frac{1}{200} \sum_{s=1}^{200} \hat{\lambda}_s - \lambda_{\text{true}} \right),$$

while relative root mean squared error (rRMSE) summarizes overall accuracy,

$$\text{rRMSE} = \frac{1}{\lambda_{\text{true}}} \sqrt{\frac{1}{200} \sum_{s=1}^{200} (\hat{\lambda}_s - \lambda_{\text{true}})^2}.$$

Precision was quantified using the relative standard deviation (rSD),

$$\text{rSD} = \frac{1}{\lambda_{\text{true}}} \sqrt{\frac{1}{199} \sum_{s=1}^{200} (\hat{\lambda}_s - \bar{\lambda})^2},$$

where $\bar{\lambda}$ is the mean estimated density across replicates.

All simulations and analyses were conducted in R. An R package is provided on GitHub: <https://>

5 Results

5.1 Performance of the estimators for simulated populations

5.1.1 CSR populations

For populations modeled by the Poisson distribution, the estimators $\hat{\lambda}_C^{(c)}$, $\hat{\lambda}_P^{(c)}$, and $\hat{\lambda}_{MLE}^{(c)}$ all produced estimates with low relative bias, demonstrating comparable and robust performance across varying density levels and nearest-neighbor orders. The $\hat{\lambda}_{DK}$ was applicable only for $\ell = 1$ and exhibited substantial positive bias at lower densities where censoring was severe. The relative performance of all methods was systematically influenced by the extreme resulting censored rate, which is defined by $n_0/(nq)$.

Table 1 presents the relative bias and precision, measured as relative standard deviation (rSD), for the four Poisson-based estimators across the simulated scenarios.

5.1.2 Non-CSR populations

For aggregated populations modeled by the Thomas process, the performance of the NBD-based censored estimators varied with both the aggregation scale (σ) and the nearest-neighbor order (ℓ). Figure 1 illustrates the relative bias (rBias) of $\hat{\lambda}_n^{(c)}$, $\hat{\lambda}_{m1}^{(c)}$, and $\hat{\lambda}_{n,MLE}^{(c)}$ across a gradient of σ values for $\ell = 1, 2$, and 3. Error bars represent the relative standard deviation (rSD).

The results indicate that when $\ell = 1$ or 2, $\hat{\lambda}_{n,MLE}^{(c)}$ was generally less biased than $\hat{\lambda}_n^{(c)}$ across most aggregation scales. At $\ell = 3$, the two estimators exhibited comparable performance in terms of bias. In terms of precision, $\hat{\lambda}_{n,MLE}^{(c)}$ and $\hat{\lambda}_n^{(c)}$ performed similarly to each other across all scenarios. However, both $\hat{\lambda}_{n,MLE}^{(c)}$ and $\hat{\lambda}_n^{(c)}$ consistently outperformed $\hat{\lambda}_{m1}^{(c)}$ in both bias and variance, with the latter showing larger deviations and greater uncertainty.

5.2 Performance on empirical forest plot data

Consistent with results from the simulated populations, the performance of the estimators on the empirical BCI data exhibited clear trends with the nearest-neighbor order ℓ . As ℓ increased from 1 to 3, the median relative bias (rBias) of most estimators systematically shifted from negative values toward zero or slightly positive values (Figure 2, left column).

Table 1: Relative bias and precision of Poisson-based estimators for simulated complete spatial randomness populations. Values are presented as rBias (rSD). **Bolded** values indicate the smallest absolute relative bias for each scenario. The symbol “—” indicates that the estimator is not applicable for the given ℓ .

Intensity	ℓ	$\hat{\lambda}_{\text{MLE}}^{(c)}$	$\hat{\lambda}_C^{(c)}$	$\hat{\lambda}_{\text{DK}}$	$\hat{\lambda}_P^{(c)}$	Censored Rate
0.005	1	-0.0035 (0.0795)	-0.0017 (0.0936)	0.5812 (0.1385)	-0.0041 (0.0884)	0.676
	2	-0.0065 (0.1060)	-0.1120 (0.1160)	—	-0.0018 (0.1240)	0.941
	3	-0.0220 (0.1850)	-0.1440 (0.2250)	—	0.0060 (0.2550)	0.992
0.010	1	-0.0052 (0.0623)	-0.0020 (0.0737)	0.4415 (0.0958)	-0.0043 (0.0689)	0.458
	2	0.0026 (0.0630)	-0.1050 (0.0682)	—	0.0051 (0.0728)	0.813
	3	0.0004 (0.0886)	-0.1430 (0.0930)	—	0.0039 (0.1050)	0.954
0.050	1	0.0005 (0.0451)	0.0011 (0.0479)	0.0425 (0.0476)	-0.0009 (0.0455)	0.020
	2	-0.0012 (0.0328)	-0.1120 (0.0309)	—	-0.0017 (0.0335)	0.098
	3	-0.0020 (0.0282)	-0.1480 (0.0258)	—	-0.0027 (0.0294)	0.250

Similar results and patterns were observed for different maximum search radius ($C = 10, 20, 30, 40$ m) and in the Harvard Forest 35-ha plot (see Appendix SM: Section S4 for more plots). Quantitatively, the NBD-based maximum likelihood estimator $\hat{\lambda}_{n,\text{MLE}}^{(c)}$ achieved a median rBias below 20% across the vast majority of species and sampling scenarios in both forest plots, a level of estimation accuracy that was not consistently attained by any of the other CSR- or NBD-based estimators evaluated in this study.

6 Discussion

This study develops a unified and systematic framework for estimating population density from PCQM data. By extending both moment-based and likelihood-based estimators under the Pois-

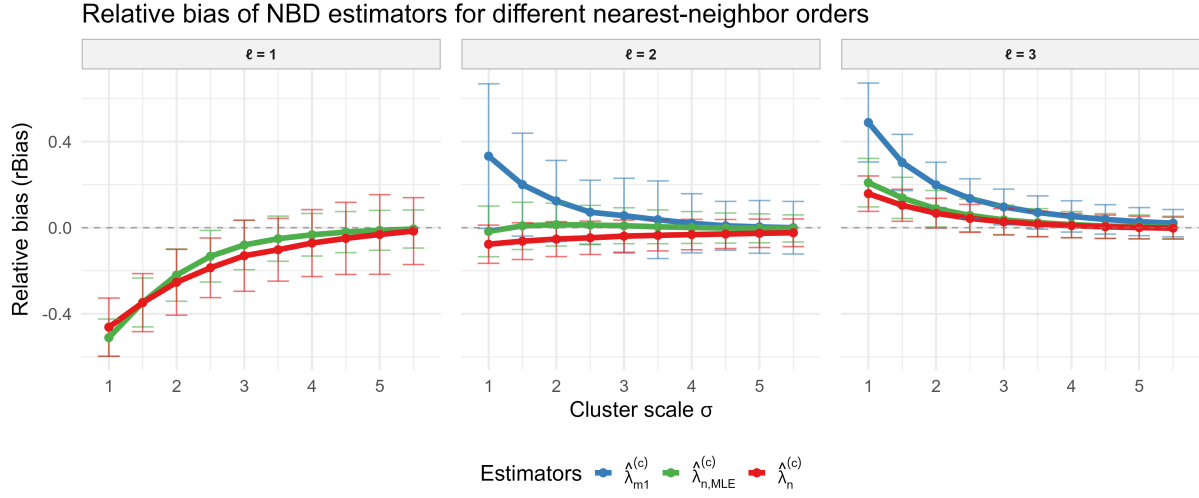


Figure 1: Relative bias (rBias, points and solid lines) of three NBD-based censored estimators, $\hat{\lambda}_n^{(c)}$ (red), $\hat{\lambda}_{m1}^{(c)}$ (blue, not applicable for $\ell = 1$), and $\hat{\lambda}_{n,MLE}^{(c)}$ (green), across a gradient of cluster scales (σ) for nearest-neighbor orders $\ell = 1, 2$, and 3. Error bars represent \pm one relative standard deviation (rSD). Simulations are based on a Thomas cluster process with intensity $\lambda = 0.05$ and censoring radius $C = 10$ m.

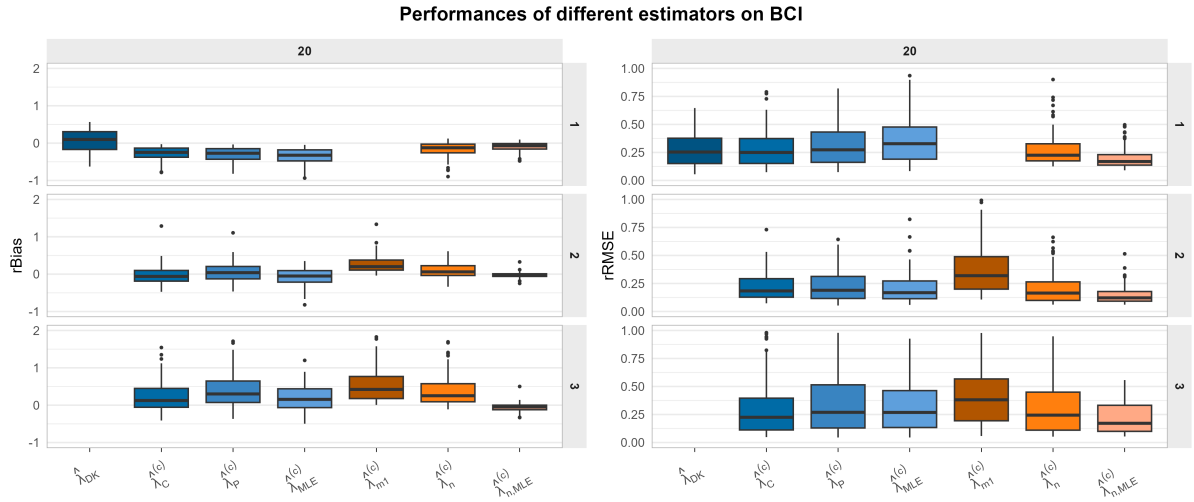


Figure 2: Performance of seven censored distance-based estimators applied to tree populations in BCI. Left column: Relative bias (rBias) across nearest-neighbor orders $\ell = 1, 2, 3$ (rows) for a fixed censoring radius $C = 20$ m. Right column: Corresponding relative root mean squared error (rRMSE). Estimators are grouped by underlying spatial assumption: Complete Spatial Randomness (CSR: $\hat{\lambda}_{DK}^{(c)}$, $\hat{\lambda}_C^{(c)}$, $\hat{\lambda}_P^{(c)}$, $\hat{\lambda}_{MLE}^{(c)}$) and Negative Binomial Distribution (NBD: $\hat{\lambda}_{m1}^{(c)}$, $\hat{\lambda}_n^{(c)}$, $\hat{\lambda}_{n,MLE}^{(c)}$). Note that $\hat{\lambda}_{m1}^{(c)}$ is not applicable for $\ell = 1$. The boxplots summarize the distribution of each metric across 200 sampling replications for 112 analyzed species (abundance ≥ 500 individuals).

son model for complete spatial randomness and the NBD model for aggregated populations, we provide a coherent set of tools applicable to realistic field conditions with a maximum search radius. Simulations and applications to forest plot data consistently showed that the NBD-based maximum likelihood estimator for censored data, $\hat{\lambda}_{n,\text{MLE}}^{(c)}$, achieves the highest accuracy and robustness when spatial aggregation is present.

A key finding concerns the practical trade-off between the maximum search radius (C) and the nearest-neighbor order (ℓ) in censored designs. While higher ℓ values generally improve estimation in uncensored sampling (Kronenfeld, 2009; Khan et al., 2016), this advantage is substantially eroded under a finite search radius. As ℓ increases, the probability of censored sectors rises sharply (see Appendix SM: Section S4). Under severe truncation (e.g., $C \leq 20$ m in our simulations), lower-order designs ($\ell = 1$ or 2) provide a more reliable balance between information content and censoring-induced bias.

From an applied standpoint, our results offer clear guidance. When populations are approximately random, Poisson-based censored estimators perform well ($\hat{\lambda}_C^{(c)}$, $\hat{\lambda}_P^{(c)}$, $\hat{\lambda}_{\text{MLE}}^{(c)}$). However, when spatial aggregation is expected—a common situation in forest ecosystems—and especially when censoring is non-negligible, the NBD-based likelihood estimator $\hat{\lambda}_{n,\text{MLE}}^{(c)}$ is recommended due to its consistently low bias and competitive precision.

Several limitations should be acknowledged. The NBD framework does not represent all possible spatial patterns, such as strong inhibition (Cogbill et al., 2018). And the moment-based censored NBD estimators ($\hat{\lambda}_n^{(c)}$, $\hat{\lambda}_{m1}^{(c)}$) rely on an initial density estimate, introducing an approximation step.

In summary, this work extends classical distance-based density estimation by jointly addressing spatial aggregation and right-censoring within a unified likelihood framework, providing a validated foundation for plotless density estimation under practical field constraints.

References

- Baddeley, A., E. Rubak, and R. Turner (2015). *Spatial Point Patterns: Methodology and Applications with R*. Boca Raton, FL: Chapman and Hall/CRC. [10]
- Carnell, R. (2026). *lhs: Latin Hypercube Samples*. R package version 1.2.1. [10]
- Chen, Y., T.-J. Shen, R. Condit, and S. P. Hubbell (2018). Community-level species' correlated distribution can be scale-independent and related to the evenness of abundance. *Ecology* 99(12), 2787–2800. [5]

- Cogbill, C. V. (2023). Surveyor and analyst biases in forest density estimation from United States public land surveys. *Ecosphere* 14(8), e4647. [2]
- Cogbill, C. V., A. L. Thurman, J. W. Williams, D. J. Mladenoff, and S. J. Goring (2018). A retrospective on the accuracy and precision of plotless forest density estimators in ecological studies. *Ecosphere* 9(2), e02187. [4, 5, 15]
- Cottam, G. and J. Curtis (1956). The use of distance measures in phytosociological sampling. *Ecology* 37(3), 451–460. [2]
- Cottam, G., J. Curtis, and B. Hale (1953). Some sampling characteristics of a population of randomly dispersed individuals. *Ecology* 34(4), 741–757. [2]
- Dahdouh-Guebas, F. and N. Koedam (2006). Empirical estimate of the reliability of the use of the point-centred quarter method (PCQM): Solutions to ambiguous field situations and description of the PCQM+ protocol. *Forest Ecology and Management* 228(1-3), 1–18. [2, 7, SM 3]
- Eberhardt, L. L. (1967). Some developments in ‘distance sampling’. *Biometrics* 23(2), 207–216. [4, 5]
- Foster, D. R. (1992). Land-use history (1730-1990) and vegetation dynamics in central new england, usa. *Journal of Ecology* 80, 753–772. [11]
- Gao, M. (2013). Detecting spatial aggregation from distance sampling: A probability distribution model of nearest neighbor distance. *Ecological Research* 28, 397–405. [5]
- He, F., P. Legendre, and J. V. LaFrankie (1997). Distribution patterns of tree species in a malaysian tropical rain forest. *Journal of Vegetation Science* 8(1), 105–114. [2]
- Hubbell, S., R. Foster, and M. Soulé (1986). Conservation biology: the science of scarcity and diversity. *Commonness and rarity in a neotropical forest: implications for tropical tree conservation*. Sinauer Associates, Massachusetts, 205–231. [11]
- Khan, M. N., R. Hijbeek, U. Berger, N. Koedam, U. Grütters, S. M. Islam, M. Hasan, and F. Dahdouh-Guebas (2016). An evaluation of the plant density estimator the point-centred quarter method (pcqm) using monte carlo simulation. *PloS one* 11, e0157985. [15]
- Kronenfeld, B. J. (2009). A plotless density estimator based on the asymptotic limit of ordered distance estimation values. *Forest Science*. [15]
- Levine, C. R., C. V. Cogbill, B. M. Collins, A. J. Larson, J. A. Lutz, M. P. North, C. M. Restaino, H. D. Safford, S. L. Stephens, and J. J. Battles (2017). Evaluating a new method

- for reconstructing forest conditions from General Land Office survey records. *Ecological Applications* 27(5), 1498–1513. [2]
- Mitchell, K. (2007). *Quantitative analysis by the point-centered quarter method*. Hobart and William Smith Colleges. [2, 6]
- Morisita, M. (1954). Estimation of population density by spacing method. *Memoirs of the Faculty of Science, Kyushu University. Series E, Biology 1*, 187–197. [2, 4]
- Morisita, M. (1957). A new method for the estimation of density by the spacing method applicable to nonrandomly distributed populations. *Physiology and Ecology* 7, 134–144. [4, 5]
- Olsson, A., G. Sandberg, and O. Dahlblom (2003). On latin hypercube sampling for structural reliability analysis. *Structural Safety* 25(1), 47–68. [10]
- Pollard, J. (1971). On distance estimators of density in randomly distributed forests. *Biometrics*, 991–1002. [2, 4]
- Santini, L., V. Y. Mendez Angarita, C. Karoulis, D. Fundarò, N. Pranzini, C. Vivaldi, T. Zhang, A. Zampetti, S. J. Gargano, D. Mirante, and L. Paltrinieri (2024). TetraDENSITY 2.0—a database of population density estimates in tetrapods. *Global Ecology and Biogeography* 33, e13929. [2]
- Shen, G., X. Wang, and F. He (2020). Distance-based methods for estimating density of non-randomly distributed populations. *Ecology* 101(10), e03143. [2, 5]
- Stoklosa, J., R. V. Blakey, and F. K. C. Hui (2022). An overview of modern applications of negative binomial modelling in ecology and biodiversity. *Diversity* 14(5). [2]
- Thomas, M. (1949). A generalization of poisson’s binomial limit for use in ecology. *Biometrika* 36(1/2), 18–25. [9, 10]
- Warde, W. and J. W. Petranka (1981). A correction factor table for missing point-center quarter data. *Ecology* 62(2), 491–494. [2, 6, SM 1, SM 3]
- Zillio, T. and F. He (2010). Modeling spatial aggregation of finite populations. *Ecology* 91(12), 3698–3706. [5]

Supplementary Materials

SM§1 Moment Adjustment for Right-Censored Data under Poisson case

This section provides a detailed derivation of the generalized moment-based density estimators for right-censored distance sampling data, extending the original work of [Warde and Petranka \(1981\)](#) from the special case of $\ell = 1$ to the general case of the ℓ -th nearest neighbor in q sectors and to other kinds of moments-based estimators.

Consider a sampling design with q equal-angle sectors per focal point. Under the assumption of complete spatial randomness (CSR) with density λ (individuals per unit area), the number of individuals m in a sector of radius r follows a Poisson distribution with parameter:

$$m = \lambda\pi r^2/q.$$

The cumulative distribution function of the distance R to the ℓ -th nearest neighbor within a sector is

$$\Pr(R \leq r) = 1 - \sum_{i=0}^{\ell-1} \frac{(\lambda\pi r^2/q)^i}{i!} e^{-\lambda\pi r^2/q}.$$

The probability density function is

$$f(r) = \frac{2\pi\lambda r}{q} \frac{(\lambda\pi r^2/q)^{\ell-1}}{(\ell-1)!} e^{-\lambda\pi r^2/q}.$$

The u -th moment of R under complete sampling is given by

$$\mathbb{E}[R^u] = \int_0^\infty r^u f(r) dr = \left(\frac{q}{\pi\lambda}\right)^{u/2} \frac{\Gamma(\ell + \frac{u}{2})}{(\ell-1)!}. \quad (\text{SM.1})$$

In truncated sampling with maximum search radius C , we only observe distances when $R \leq C$. The probability of observing at least ℓ individuals within radius C is

$$P = 1 - \sum_{i=0}^{\ell-1} \frac{m_C^i}{i!} e^{-m_C}, \quad \text{where } m_C = \lambda\pi C^2/q.$$

Practically, P is estimated by the observed proportion of non-censored sectors: $\hat{P} = 1 - n_0/(nq)$. The conditional u -th moment given $R \leq C$ is

$$\mathbb{E}[R^u \mid R \leq C] = \frac{\int_0^C r^u f(r) dr}{P}.$$

The numerator is

$$\int_0^C r^u f(r) dr = \frac{2\pi\lambda}{q} \frac{(\lambda\pi/q)^{\ell-1}}{(\ell-1)!} \int_0^C r^{2\ell+u-1} e^{-br^2} dr,$$

where $b = \lambda\pi/q$.

Using the substitution $t = br^2$ and the definition of the lower incomplete gamma function $\gamma(s, x) = \int_0^x t^{s-1} e^{-t} dt$, we obtain

$$\int_0^C r^{2\ell+u-1} e^{-br^2} dr = \frac{1}{2} b^{-(\ell+u/2)} \gamma\left(\ell + \frac{u}{2}, m_C\right).$$

Therefore,

$$\int_0^C r^u f(r) dr = \frac{\gamma\left(\ell + \frac{u}{2}, m_C\right)}{(\ell-1)!} \left(\frac{q}{\pi\lambda}\right)^{u/2}.$$

The conditional moment becomes

$$\mathbb{E}[R^u | R \leq C] = \frac{\gamma\left(\ell + \frac{u}{2}, m_C\right)}{(\ell-1)!P} \left(\frac{q}{\pi\lambda}\right)^{u/2}. \quad (\text{SM.2})$$

Comparing with the unconditional moment $\mathbb{E}[R^u]$ (SM.1), we establish the relationship:

$$\mathbb{E}[R^u] = \mathbb{E}[R^u | R \leq C] \cdot \frac{\Gamma\left(\ell + \frac{u}{2}\right)}{\gamma\left(\ell + \frac{u}{2}, m_C\right)} \cdot P.$$

In practice, we compute the sample conditional moment $\widehat{M}_u = \frac{1}{nq-n_0} \sum_{t=1}^{nq-n_0} r_t'^u$ from the $nq - n_0$ non-censored observations. The adjusted unconditional moment estimator is therefore

$$M_u = \widehat{M}_u \cdot \frac{\Gamma\left(\ell + \frac{u}{2}\right)}{\gamma\left(\ell + \frac{u}{2}, \widehat{m}_C\right)} \cdot \widehat{P},$$

where \widehat{m}_C is the solution to $\frac{\gamma(\ell, \widehat{m}_C)}{\Gamma(\ell)} = \widehat{P}$, providing an estimate of m_C , since

$$\frac{\gamma(\ell, x)}{\Gamma(\ell)} = 1 - \sum_{k=0}^{\ell-1} \frac{x^k}{k!} e^{-x}.$$

SM§2 Theoretical Justification for Moment Adjustment under NBD Model

SM§2.1 Why is the Adjusted Moment $\widehat{\mathbb{E}[R^u]}$ Justified?

For a sampling design with n focal points, each divided into q equal-angle sectors, we measure distances R_j ($j = 1, \dots, nq$) to the ℓ -th nearest individual. A maximum search radius C results in right-censored observations ($R_j > C$). The adjusted u -th sample moment is

$$\widehat{\mathbb{E}[R^u]} \approx \frac{1}{nq} \sum_{j=1}^{nq} [\mathbb{1}_{\{R_j \leq C\}} R_j^u + \mathbb{1}_{\{R_j > C\}} \mathbb{E}[R^u \mid R > C; k = +\infty, \lambda = \lambda_{\text{init}}]],$$

where $\mathbb{1}_{\{\cdot\}}$ is the indicator function, and $\mathbb{E}[R^u \mid R > C; k = +\infty, \lambda = \lambda_{\text{init}}]$ is the conditional expectation under the CSR assumption ($k = +\infty$) with an initial density estimate λ_{init} , typically from traditional methods (Warde and Petranka, 1981; Dahdouh-Guebas and Koedam, 2006) or our generalized estimator. The CSR conditional expectation is

$$\mathbb{E}[R^u \mid R > C; k = +\infty, \lambda = \lambda_{\text{init}}] = (\pi \lambda_{\text{init}} q^{-1})^{-u/2} \frac{\Gamma(\ell + \frac{u}{2}, \pi \lambda_{\text{init}} q^{-1} C^2)}{\Gamma(\ell, \pi \lambda_{\text{init}} q^{-1} C^2)},$$

where $\Gamma(a, x)$ is the upper incomplete gamma function $\Gamma(a, x) = \int_x^\infty t^{a-1} e^{-t} dt$.

This formulation is justified by the Strong Law of Large Numbers (SLLN). If the true parameters k, λ were known, we define

$$Z_j = \mathbb{1}_{\{R_j \leq C\}} R_j^u + \mathbb{1}_{\{R_j > C\}} \mathbb{E}[R^u \mid R > C; k, \lambda],$$

with $\mathbb{E}[Z_j] = \mathbb{E}[R^u]$. By the SLLN, $\frac{1}{nq} \sum_{j=1}^{nq} Z_j \rightarrow \mathbb{E}[R^u]$. Since the true parameters are unknown, we approximate them with $k = +\infty$ and λ_{init} . The bias can be estimated by

$$\begin{aligned} \text{Bias} &\approx \Pr(R > C) \cdot [\mathbb{E}[R^u \mid R > C; k = +\infty, \lambda = \lambda_{\text{init}}] - \mathbb{E}[R^u \mid R > C; k, \lambda]] \\ &\approx \Pr(R > C) \cdot [\mathbb{E}[R^u \mid R > C; k = +\infty, \lambda = \lambda] - \mathbb{E}[R^u \mid R > C; k, \lambda]] \end{aligned}$$

where

$$\Pr(R > C) = 1 - I_w(\ell, k),$$

and

$$\mathbb{E}[R^u \mid R > C; k, \lambda] = \left(\frac{kq}{\pi\lambda}\right)^{u/2} \frac{\Gamma(\ell + \frac{u}{2}) \Gamma(k - \frac{u}{2})}{\Gamma(\ell)\Gamma(k)} \cdot \frac{1 - I_w(\ell + \frac{u}{2}, k - \frac{u}{2})}{1 - I_w(\ell, k)},$$

with $a = \pi \lambda q^{-1}$, $u_C = \frac{aC^2}{k}$, $w = \frac{u_C}{1+u_C}$, and $I_w(a, b)$ is the regularized incomplete Beta function.

When k is small (i.e., approaching the theoretical lower bound of $k > \frac{u}{2}$ from above) and C is relatively large, the probability $\Pr(R > C) = 1 - I_w(\ell, k)$ tends to 0. This is because $u_C = \frac{aC^2}{k}$ becomes large, causing $w = \frac{u_C}{1+u_C}$ to approach 1, and thus $I_w(\ell, k) \rightarrow 1$. Consequently, the bias term is dominated by $\Pr(R > C)$ and becomes negligible.

When k is large, the difference in conditional expectations, $\mathbb{E}[R^u \mid R > C; k = +\infty, \lambda = \lambda] - \mathbb{E}[R^u \mid R > C; k, \lambda]$, is of order $O(1/k)$. This can be rigorously shown via a Taylor expansion: for general ℓ and u (with $k > \frac{u}{2}$ to ensure the moments exist), the conditional expectation under NBD can be expanded as

$$\mathbb{E}[R^u \mid R > C; k, \lambda] = \mathbb{E}[R^u \mid R > C; k = +\infty, \lambda = \lambda] + \frac{\Delta_1}{k} + O\left(\frac{1}{k^2}\right),$$

where $\mathbb{E}[R^u \mid R > C; k = +\infty, \lambda = \lambda] = a^{-u/2} \frac{\Gamma(\alpha, T)}{\Gamma(\ell, T)}$ with $a = \pi \lambda q^{-1}$, $\alpha = \ell + \frac{u}{2}$, and $T = aC^2$, and Δ_1 is an explicit constant given by

$$\Delta_1 = a^{-u/2} \frac{-\ell \Gamma(\alpha + 1, T) \Gamma(\ell, T) + \frac{1}{2} \Gamma(\alpha + 2, T) \Gamma(\ell, T) + \ell \Gamma(\alpha, T) \Gamma(\ell + 1, T) - \frac{1}{2} \Gamma(\alpha, T) \Gamma(\ell + 2, T)}{\Gamma(\ell, T)^2}.$$

Thus, the difference vanishes as k increases, confirming the robustness of the approximation.

SM§2.2 Why is the Adjusted Moment $\widehat{\mathbb{E}[R^u]}$ Better than M_u ?

We characterize the asymptotic behavior of $\widehat{\mathbb{E}[R^u]}$ and M_u as the total number of sampled sectors $N = nq \rightarrow \infty$ (i.e., the sample size n of focal points tends to infinity).

Asymptotic Limit of M_u . When $N \rightarrow \infty$, the empirical censoring proportion $p_0^{\text{obs}} = n_0/N$ converges to the theoretical censoring probability $p_0 = 1 - \Pr(R \leq C; \lambda, k)$, where $\Pr(R \leq C; \lambda, k) = I_w(\ell, k)$. The Poisson-based adjusted moment M_u converges to its asymptotic limit:

$$M_u^\infty = \mathbb{E}[R^u \mid R \leq C; \lambda, k] \cdot \frac{\Gamma\left(\ell + \frac{u}{2}\right)}{\gamma\left(\ell + \frac{u}{2}, \widehat{m}_C^\infty\right)} \cdot (1 - p_0),$$

where \widehat{m}_C^∞ is the solution to $\gamma(\ell, \widehat{m}_C^\infty)/\Gamma(\ell) = 1 - p_0$ and $\mathbb{E}[R^u \mid R \leq C; \lambda, k]$ is the theoretical conditional expectation of R^u given $R \leq C$ under the NBD model.

Asymptotic Limit of $\widehat{\mathbb{E}[R^u]}$. For the censored-adjusted moment $\widehat{\mathbb{E}[R^u]}$ (tailored for the NBD model), as $N \rightarrow \infty$, the initial density estimate λ_{init} (derived from the Pollard-type censored

estimator) converges to its theoretical value $\lambda_{\text{init}}^\infty = \frac{\ell q}{\pi M_2^\infty}$. Consequently, $\widehat{\mathbb{E}[R^u]}$ converges to

$$\widehat{\mathbb{E}[R^u]}^\infty = (1 - p_0) \cdot \mathbb{E}[R^u \mid R \leq C; \lambda, k] + p_0 \cdot \mathbb{E}[R^u \mid R > C; \lambda_{\text{init}}^\infty, k \rightarrow \infty],$$

where $\mathbb{E}[R^u \mid R > C; \lambda_{\text{init}}^\infty, k \rightarrow \infty]$ denotes the theoretical conditional expectation of R^u given $R > C$ under CSR with density $\lambda_{\text{init}}^\infty$.

Asymptotic Bias Comparison. Let $\mu_u^* = \mathbb{E}[R^u]$ be the true u -th moment of R under the uncensored NBD model. The asymptotic bias of M_u is defined as $B(M_u) = M_u^\infty - \mu_u^*$, and the asymptotic bias of $\widehat{\mathbb{E}[R^u]}$ is $B(\widehat{\mathbb{E}[R^u]}) = \widehat{\mathbb{E}[R^u]}^\infty - \mu_u^*$.

We evaluated the bias across an extensive set of parameter combinations:

- Nearest neighbor order: $\ell \in \{1, 2, 3, 4, 5, 6\}$,
- Number of angular sectors: $q \in \{1, 2, 3, 4\}$,
- Population density: $\lambda \in \{0.001, 0.006, 0.011, \dots, 2.001\}$ (step size 0.005),
- Aggregation parameter: $k \in \{0.5, 1.0, 1.5, \dots, 10\}$ (step size 0.5),
- Truncation radius: $C \in \{5, 10, 20, 30, 40, 50\}$,
- Moment order: $u \in \{-2, -1, 1, 2\}$.

For all valid parameter combinations (satisfying $k > u/2$), the absolute asymptotic bias of $\widehat{\mathbb{E}[R^u]}$ is strictly smaller than that of M_u (i.e., $|B(\widehat{\mathbb{E}[R^u]})| < |B(M_u)|$).

SM§3 Empirical Performance Across Varying Censoring Radii and Forest Plots

This section provides supplementary figures showing the performance of the seven censored density estimators under different maximum search radii C for both the Barro Colorado Island (BCI) 50-ha plot and the Harvard Forest 35-ha plot. The figures complement the results presented in the main text by illustrating patterns observed at additional censoring radii ($C = 20, 30, 40$ m). Results are summarized from 200 independent sampling replications for all species meeting the analysis threshold (BCI: 121 species; Harvard Forest: 20 species; each with ≥ 500 individuals). The mean censored rate (i.e., the proportion of sampling sectors where less than ℓ individuals were detected within radius C) is also reported under each setting.

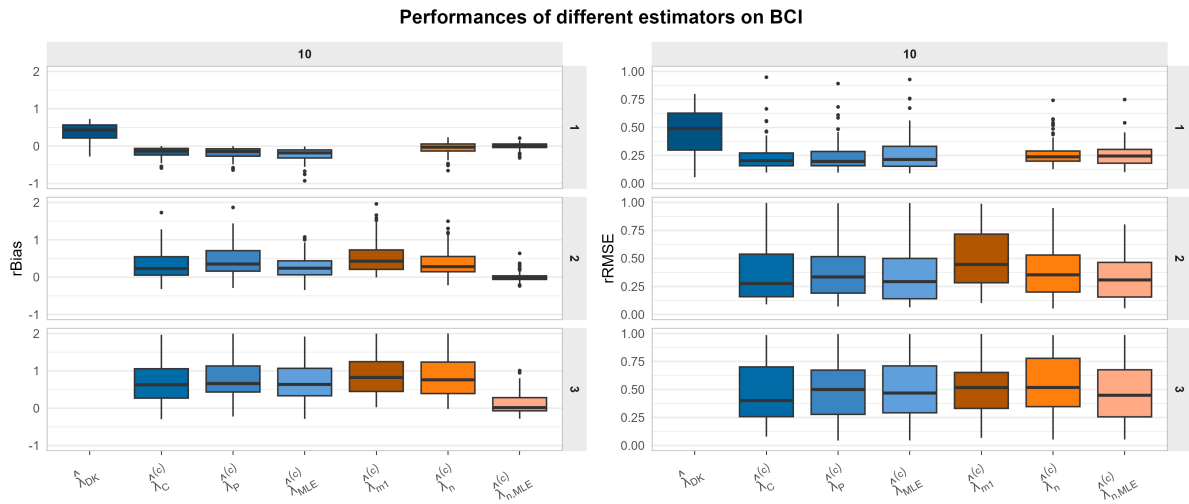


Figure SM.1: Performance of the seven estimators for the Barro Colorado Island (BCI) plot with a maximum search radius $C = 10$ m. Left column: Relative bias (rBias); Right column: Relative root mean squared error (rRMSE). Rows from top to bottom correspond to $\ell = 1, 2, 3$, respectively.

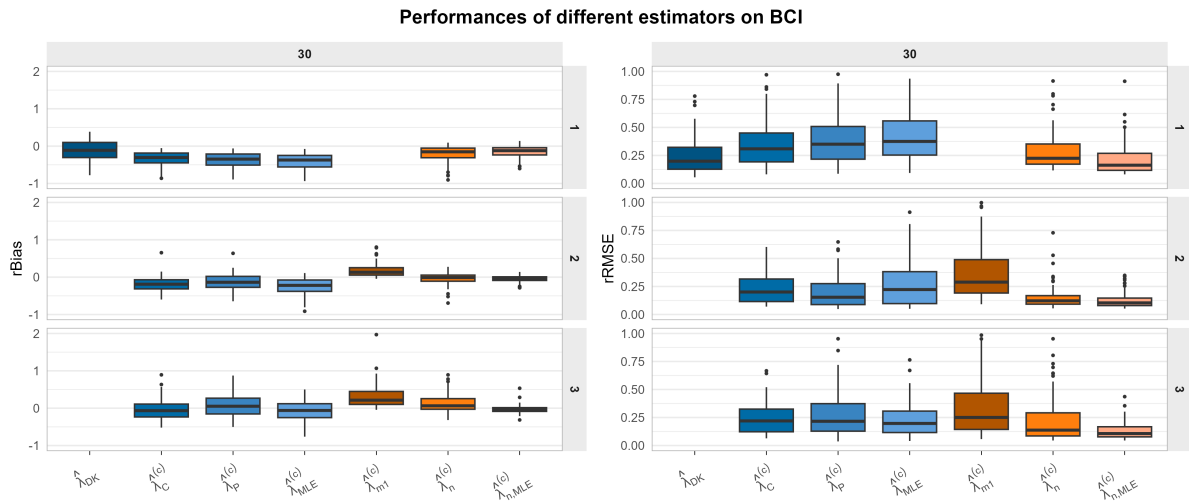


Figure SM.2: Performance of the seven estimators for the Barro Colorado Island (BCI) plot with a maximum search radius $C = 30$ m. Layout is identical to Figure SM.1.

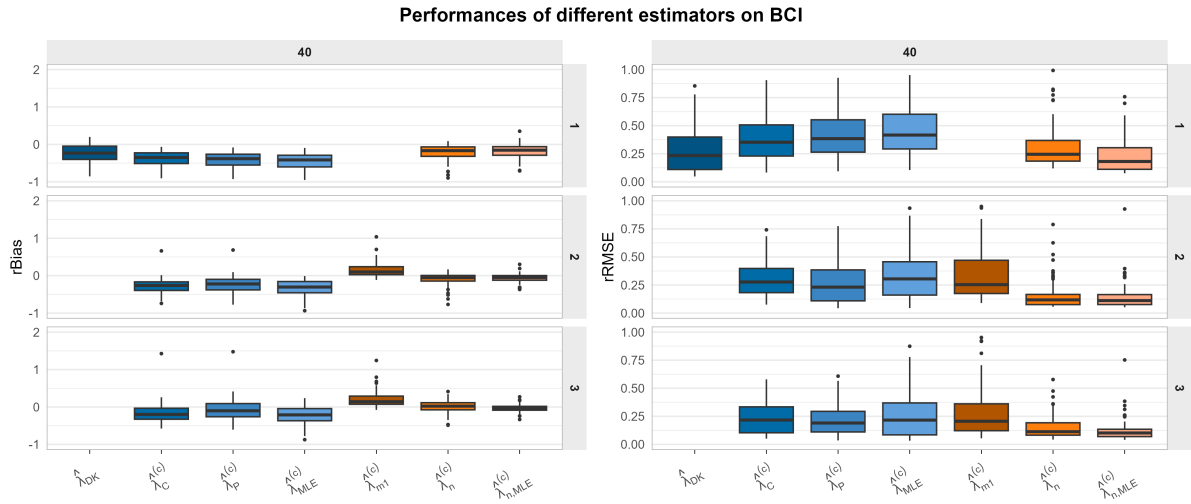


Figure SM.3: Performance of the seven estimators for the Barro Colorado Island (BCI) plot with a maximum search radius $C = 40$ m. Layout is identical to Figure SM.1.

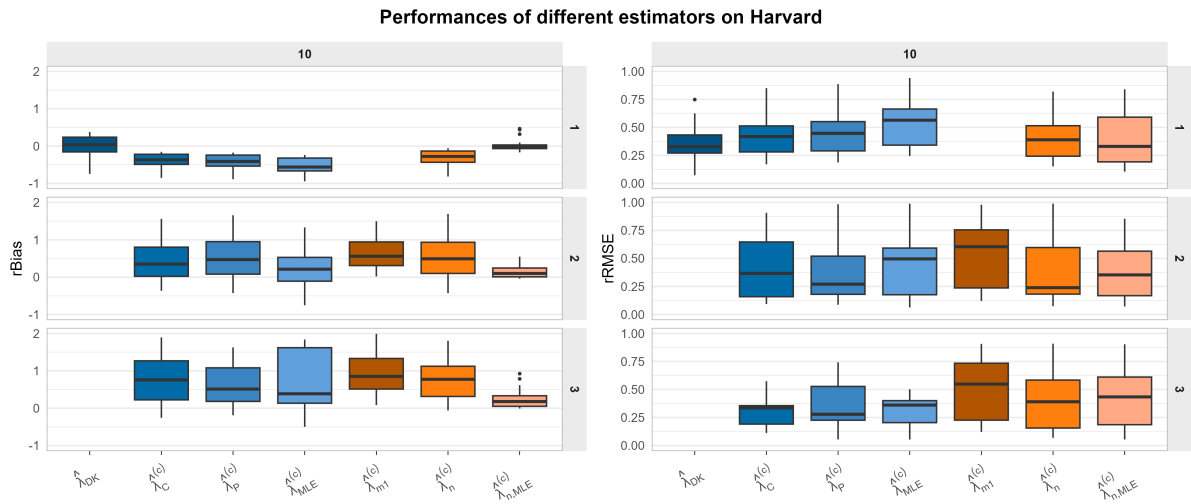


Figure SM.4: Performance of the seven estimators for the Harvard Forest plot with a maximum search radius $C = 10$ m. Layout is identical to Figure SM.1.

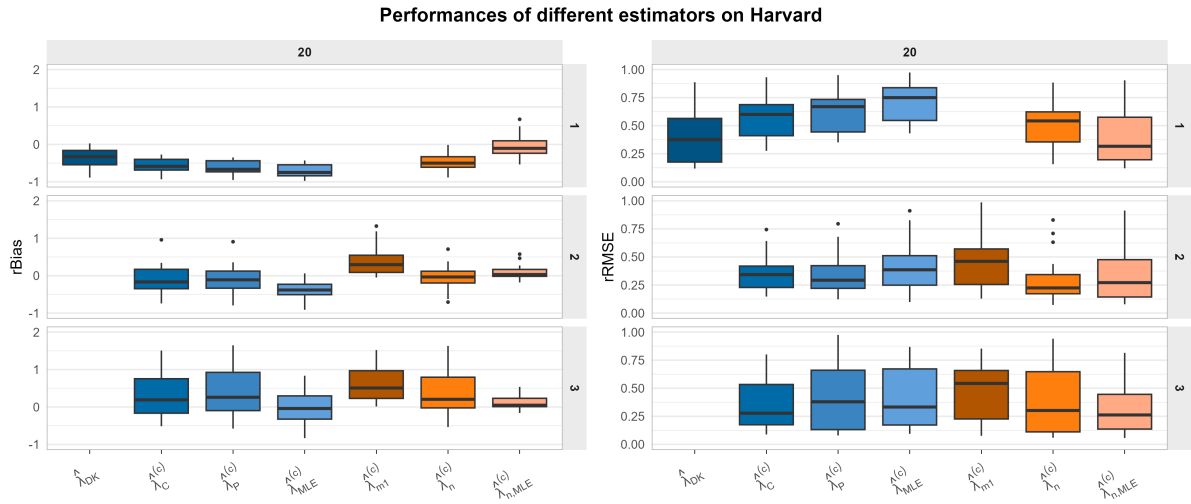


Figure SM.5: Performance of the seven estimators for the Harvard Forest plot with a maximum search radius $C = 20$ m. Layout is identical to Figure SM.1.

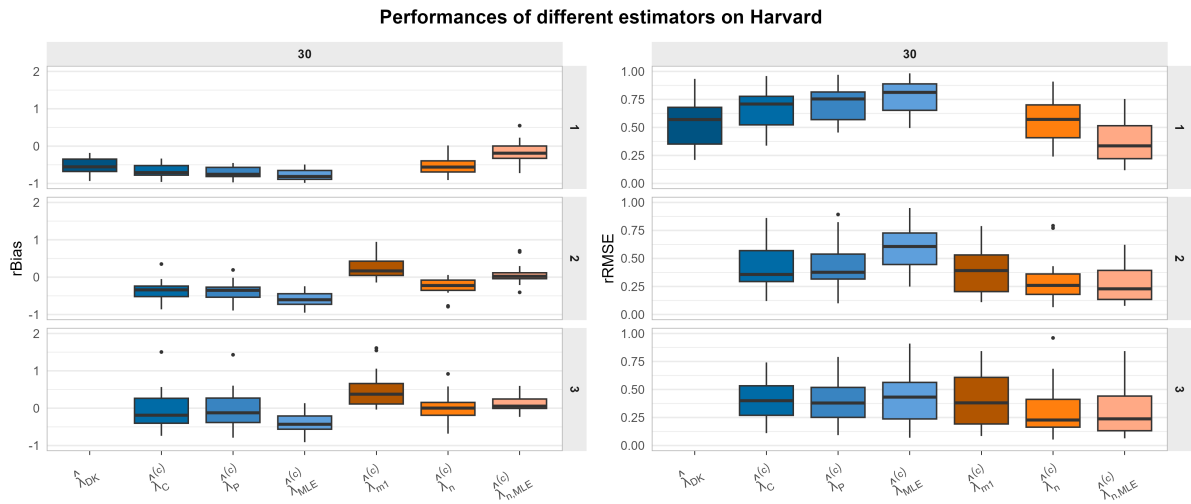


Figure SM.6: Performance of the seven estimators for the Harvard Forest plot with a maximum search radius $C = 30$ m. Layout is identical to Figure SM.1.

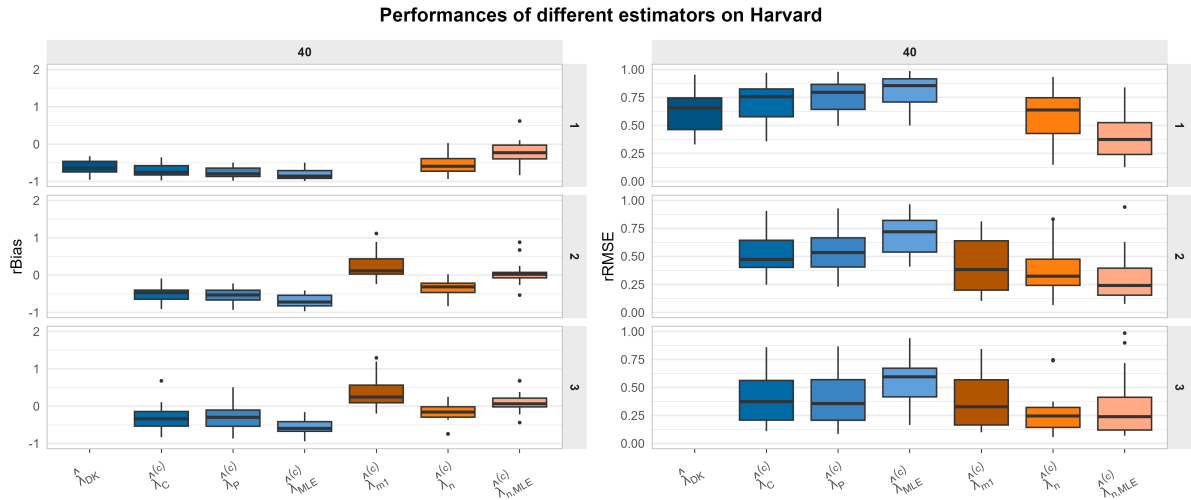


Figure SM.7: Performance of the seven estimators for the Harvard Forest plot with a maximum search radius $C = 40$ m. Layout is identical to Figure SM.1.

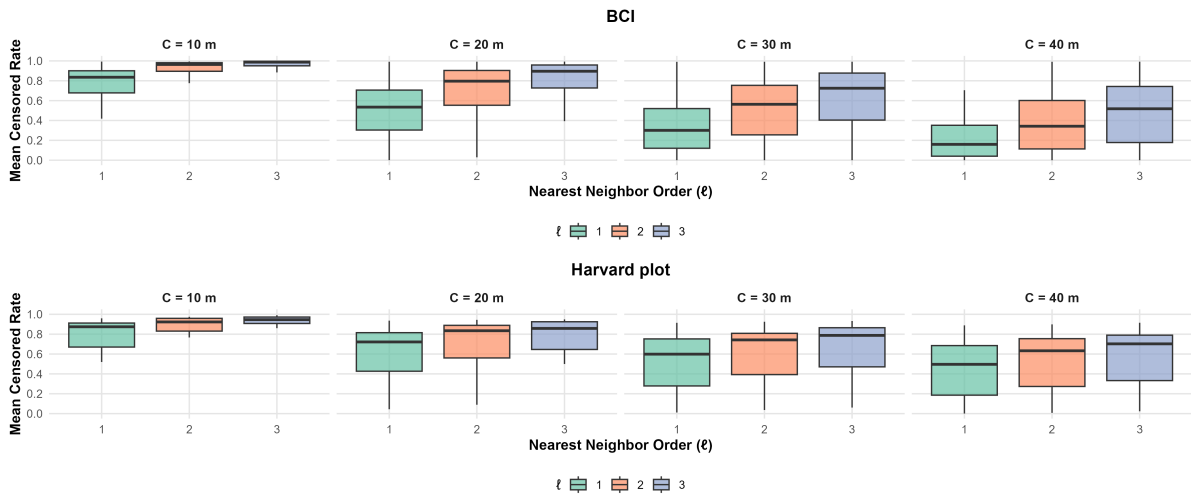


Figure SM.8: Distribution of mean censored rates under varying nearest-neighbor orders ($\ell = 1, 2, 3$) and maximum search radii ($C = 10, 20, 30, 40$ m) for the Barro Colorado Island (BCI, upper panels) and Harvard Forest plot (lower panels). Each boxplot summarizes the mean censored rate (the proportion of sampling sectors where less than ℓ individuals were detected within radius C) across 200 independent sampling replications for all analyzed species (BCI: 121 species; Harvard Forest: 20 species; each with ≥ 500 individuals).